MICRO-DAMAGE EVOLUTION IN HYBRID CARBON/STEEL KNITTED AND WOVEN FABRIC COMPOSITES

Anish N. Kulkarni[1], Andrejs Pupurs[1], Alens Šņepsts[1] and Mārtiņš Irbe[1]

[1] Laboratory of Experimental Mechanics of Materials, Ķīpsalas Street 6B-525, Riga Technical University, Riga, Latvia, LV-1048
[1] anish-niranjan.kulkarni@rtu.lv, https://ortus.rtu.lv/science/en/experts/38852

Keywords: Fabric composites, Hybrid composites, Micro-damage, Carbon fibers, Composite-metal joints

ABSTRACT

Composites with fabric reinforcements offer excellent energy dissipation and high damage tolerance as compared to long fiber unidirectional composites. Their mechanical behavior depends on local stress fields generated due to complex fabric meso-structure. Under loading, microdamage can initiate at multiple locations in this meso-structure. Thus, the design of fabric reinforcements should be carefully considered to achieve desired mechanical properties. In this work, hybrid fabric reinforcements are designed with carbon- and stainless steel fibers to be used at composite-metal joints in structural applications to achieve a smooth property gradient from the composite-side to the metal-side in such joints. Hybrid composite test specimens are subjected to quasi-static tensile loading and their properties are compared with non-hybrid carbon- and steel fiber reference materials. Their polished edges are inspected under optical microscope to detect sites of micro-damage initiation in the hybrid meso-structure. Damage propagation and corresponding stiffness reduction is also studied with increase in applied strain levels.

1 INTRODUCTION

Since the last few decades, there has been an increase in the use of knitted and woven fabric composites in aerospace and automotive industries due to their benefits over metals and UD composite tapes. Fabric composites offer ease in handling and greater flexibility in processing than UD tapes [1-8]. They also offer excellent damage tolerance at moderate costs as compared to UD composites and great weight savings at the same performance as compared to metals [2, 4-9]. However, due to significant crimp in the yarns [3, 7], modulus and strength are lower for fabric composites than UD composites.

Material properties of fabric composites are highly dependent on their textile meso-structure [1, 7-8]. It has been shown that meso-structure of fibrous yarns is the main deciding factor for nature of micro-damage than can initiate in these materials upon mechanical loading [7]. Between knitted and woven fabric composites, predicting mechanical behavior of knitted composites is more difficult due to large complexity in their meso-structure. Micro-damage initiation is governed by local stress state during loading. Knitted composites have a high degree of yarn curvature which generates a complex stress state [10]. This makes it difficult to predict the location of micro-damage initiation with the help of analytical models. Thus, conducting physical experiments and characterizing micro-damage becomes a necessity to study mechanical behavior of such materials in detail.

Previously, researchers have used various methods to detect microdamage in fabric composites [9], among which the prominent ones are described here briefly. The method of acoustic emission has been used to identify changes in damage modes by detecting change in the energy released while cracking. Digital image correlation has been used for strain mapping by detecting changes in speckle dot patterns on the surface of test specimens. The main drawback of these methods is they must be followed by X-ray or ultrasonic scanning for an accurate identification of damage mode. In the present work, we have used optical microscopy as the tool to study micro-damage by observing polished edges of test

specimens under optical microscope and to study nature of fiber-matrix interface by observing fracture surfaces under high-resolution scanning electron microscope.

Incorporation of metals into fiber composites started with fiber metal laminates (FMLs) which were prepared by interlacing metal layers with fiber reinforced resins or adhesives [11]. Such hybrids were designed to combine benefits of both the material classes and thereby having mechanical properties superior to composites and metals. But the weak interfacial bond between polymeric composites and metals would cause delaminations in these hybrid materials under fatigue loading. Various efforts have been made to increase the bond strength between composites and metals including adhesive bonding, bolting, and welding. Among these efforts, bolting creates stress concentrations and can also cause fiber breakage initiating further damage [12, 13]. Adhesive bonding requires higher costs and additional surface treatments for better lap shear strength [14]. Welding can be effective, but it becomes costly and time consuming with complex processing demands [13].

To counter these issues, as reported in our previous work [15], hybrid composites are developed with stainless steel fibers and carbon fibers gradually inter-woven or -knitted to form a complex fabric meso-structure reinforcing epoxy resin. Such materials, with mechanical properties intermediate between carbon-fiber epoxy (CF/EP) textile composite and steel-fiber epoxy (SF/EP) textile composite, would offer a smooth property gradient when used at a metal-composite joint. The reader is directed to our previous publication [15] to know details about manufacturing of fabrics and hybrid composites and pilot test results. In the current work, mechanical properties of these hybrids under quasi-static tensile loading and study of initiation and propagation of micro-damage are reported.

2 MATERIALS AND METHODS

In the present study, fabric reinforcements in composite materials were either knitted or woven. Plain weft knitting was performed on manual knitting machines by Brother (Japan). Weaving was performed on manual weaving machines in plain weave pattern. Yarns used were carbon fiber yarn T300B-3K-50B by Toray (France) and steel fiber yarn SY 11/1 by Fujibo (Japan) / Bekaert (Belgium). In the carbon fiber yarns, individual fiber diameter was 7 μm. In the case of steel fiber yarns, individual fiber diameter was 12 μm. CF/EP and SF/EP reference composite plates and hybrid CF/EP-SF/EP composite plates were manufactured by vacuum infusion of epoxy resin into the fabric reinforcements. The resin used was epoxy LY1564 with XB 3404-1 hardener by Huntsman (USA). The types of composite plates along with their notations and layups are listed in Tables 1-2.

Notation	Type	Lay-up
C1	Reference – CF/EP	$[(T300)_8]$
M1	Reference – SF/EP	$[(SY\ 11/1)_8]$
M2	Reference – SF/EP	$[(SY\ 11/1\ 3filaments)_8]$
H1	Hybrid	$[(Hybrid\ SY11/1+T300)_8]$
H2	Hybrid	$[(T300/SY11/1)]_{2s}$

Table 1: Knitted composites

Notation	Type	Lay-up
C4	Reference – CF/EP	$[T300\ FR\ 1x]_4$
M4	Reference – SF/EP	$[SY\ 11/1\ 2x]_3$
M5	Reference – SF/EP	$[SY\ 11/1\ 2x]_4$
H5	Hybrid	$[T300\ FR\ 1x + SY\ 11/1\ 2x]_4$

H6	Hybrid	$[SY\ 11/1\ 2x + T300\ FR\ 1x]_4$
H7	Hybrid	$[T300\ FR\ 1x + SY\ 11/1\ 2x]5 + [SY\ 11/1\ 2x + T300\ FR\ 1x]_5$
H8	Hybrid	$[(SY\ 11/1\ 2x + T300\ FR\ 1x)(T300\ FR\ 1x + SY\ 11/1\ 2x)]_{2.5}$
H9	Hybrid	$[T300\ FR\ 1x / SY\ 11/1\ 2x]_{2.5}$

Table 2: Woven composites

Square-sized specimens with dimensions 25 mm x 25 mm (length and width) were cut from each plate for fiber volume fraction studies. Fiber weight fraction and volume fraction were measured by burning off matrix in a closed box-type furnace at 400ºC. In this process, composite specimens were kept inside the furnace for 180 minutes, and their weights before and after the process were recorded. Weight fraction was converted to volume fraction with the help of individual yarn densities of carbon- and steel fiber yarn. The resultant fiber volume fractions for each composite type are shown in Fig. 1.

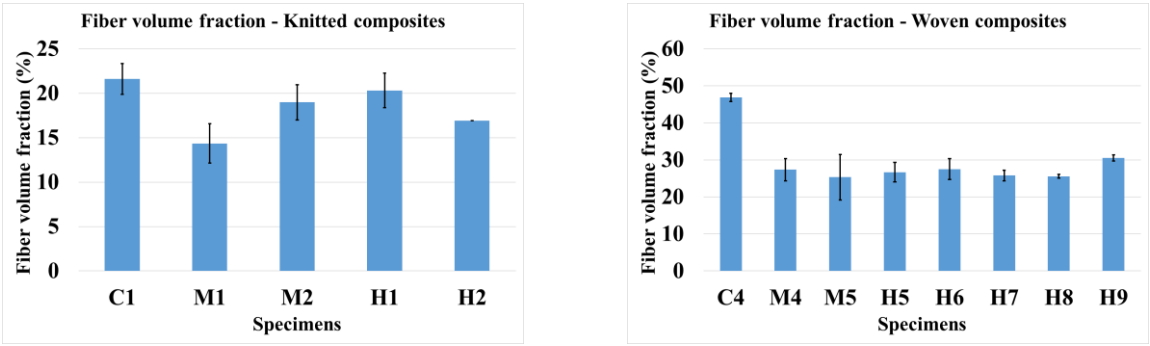

Figure 1: Fiber volume fraction – Knitted and woven composites

Rectangular specimens of 25 mm width and 200 mm length were cut from the composite plates for tensile testing and their edges were polished using manual polishing machine QATM Qpol 300 M2. The polished edges were observed under Motic 310Met optical microscope at 50x magnification to identify meso-structure of the fabric reinforcements. The meso-structures of hybrid composites are shown in Fig. 2-3.

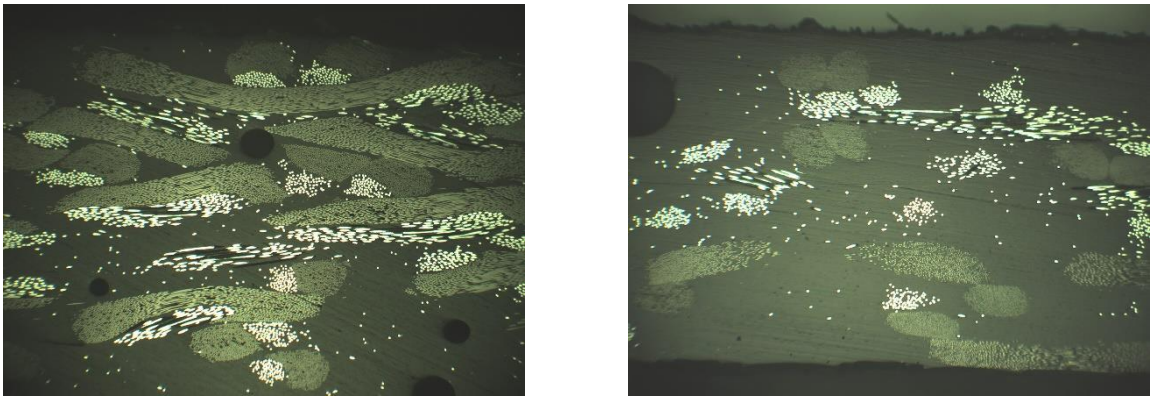

(a) (b)

Figure 2: Meso-structures of knitted composites, (a) **H1** [8 layers, with each layer of hybrid yarns] and (b) **H2** [with 4 layers CF and 4 layers SF]. Note that fibers with darker shade are carbon fibers and fibers with lighter shade are steel fibers.

Reinforcement tabs were glued on both ends of rectangular test specimens using a two-component aerospace grade adhesive from Huntsman (USA). The specimens were tested in Zwick/Roell Z150 universal testing machine under quasi-static tensile loading. Non-contact-type video extensometer MESSPHYSIK ME 46-NG and contact-type extensometer HBM Strain Link DD1 were used for strain measurements.

During quasi-static tensile loading, all the specimens were initially loaded up to 0.4% strain with 1.5 mm/min strain rate and then unloaded to zero strain with 2 mm/min strain rate. During this first loading-unloading cycle, the undamaged material modulus was measured. Following the undamaged modulus measurements, specimens were subjected to repetitive loading-unloading cycles with an increase of 0.2% in the maximum applied strain during each cycle. Between each test cycle, the polished edges were inspected in Motic 310Met optical microscope to detect presence of microdamage due to tensile loading. Stiffness was measured for each specimen during the unloading interval of each cumulative test cycle. The reduction in stiffness with increase in maximum applied strain was correlated with microdamage accumulation inside composite specimens. After final failure, fracture surfaces of failed specimens were observed under JEOL JSM IT-300 Environmental SEM to study similarities and differences in fiber fracture and nature of fiber-matrix interface for carbon- and steel fibers.

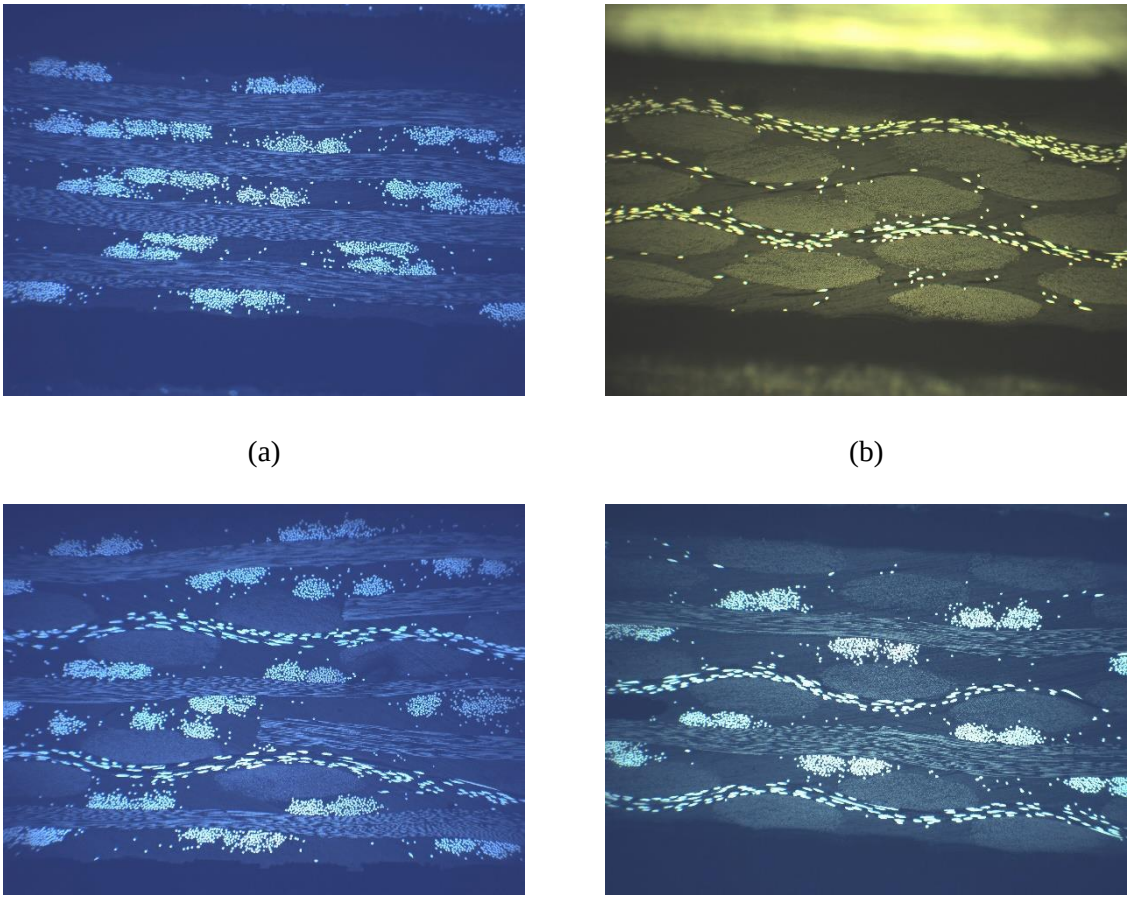

(a) (b)

(c) (d)

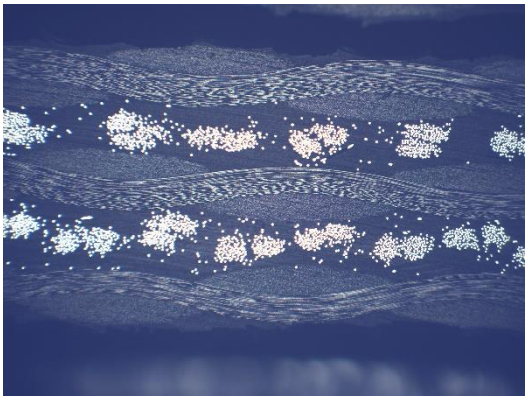

For all micrographs,

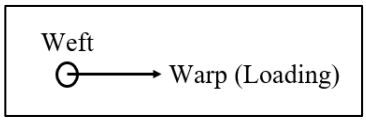

(e)

Figure 3: Meso-structures of woven composites, (a) **H5** [4 layers, with each layer of CF warp + SF weft], (b) **H6** [4 layers, with each layer of SF warp + CF weft], (c) **H7** [with 3 layers H5 & 2 layers H6], (d) **H8** [with 3 layers H6 & 2 layers H5] and (e) **H9** [with 3 layers CF & 2 layers SF]. Note that fibers with darker shade are carbon fibers and fibers with lighter shade are steel fibers.

3 RESULTS AND DISCUSSIONS

3.1 Elastic modulus measurements

The comparison of elastic moduli along the loading direction measured during the first loading-unloading cycle in quasi-static tensile testing is given in Fig. 4. In the case of knitted composites, H1 with hybrid CF-SF yarn has modulus intermediate to CF/EP reference materials C1 and SF/EP reference materials M1 and M2. H2 with alternate CF & SF layers has modulus equivalent to SF/EP reference materials. Comparing modulus values of H1 and H2, yarn hybridization gives better results than layer hybridization in the case of knitted composites.

In the case of woven composites, H5 with CF yarns in warp direction has modulus similar to CF/EP reference material C4. A similar relation can be found out with H6 and SF/EP reference materials, where H6 has SF yarns are in warp direction. This clearly indicates that for hybrid woven composites, materials used in warp/weft direction almost entirely affect the material modulus in the respective directions. In the case of hybrid compositions H7-H9, both CF and SF were used in warp yarns. Thus, their moduli are intermediate to CF/EP and SF/EP reference materials. Comparing moduli of H7 and H8, the latter has two layers with CF warp in comparison with H7 having three layers of CF warp. This reflects in the results, with H8 having lower modulus in warp direction than H7.

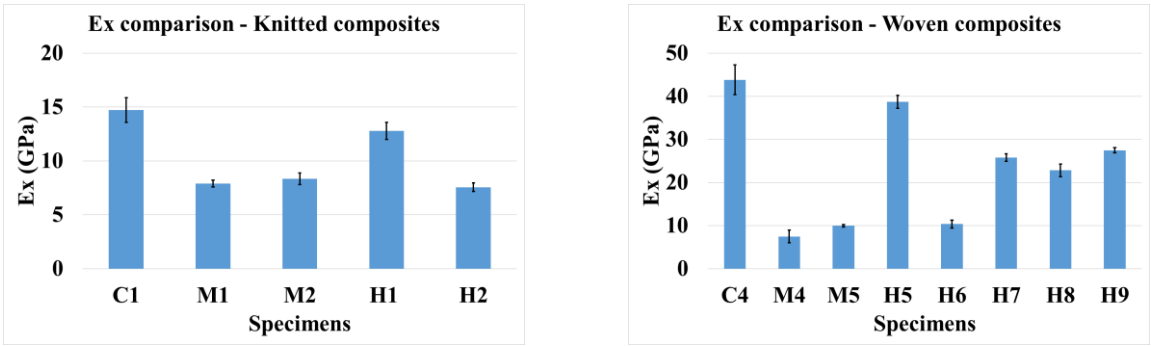

Figure 4: E (undamaged) along the loading direction – Knitted and woven composites

3.2 Micro-damage initiation and propagation – Knitted composites

Modulus measurements for undamaged materials were followed by further loading-unloading cycles with increasing levels of maximum applied strains. In the case of knitted composites, debondings in fiber-matrix interface started appearing at 0.6% maximum applied strain. Damage initiation in CF/EP reference materials as well as hybrid composites was characterized by transverse and shear cracks along weft yarn boundaries. This is shown in Fig. 5. Note that in yarn-hybrid H1, damage starts at CF yarn boundaries which then propagates along SF yarns at higher applied strain values (refer Fig. 6). Knitted hybrids show interconnecting cracks (refer Fig. 6) depicting damage propagation with increasing applied strain values.

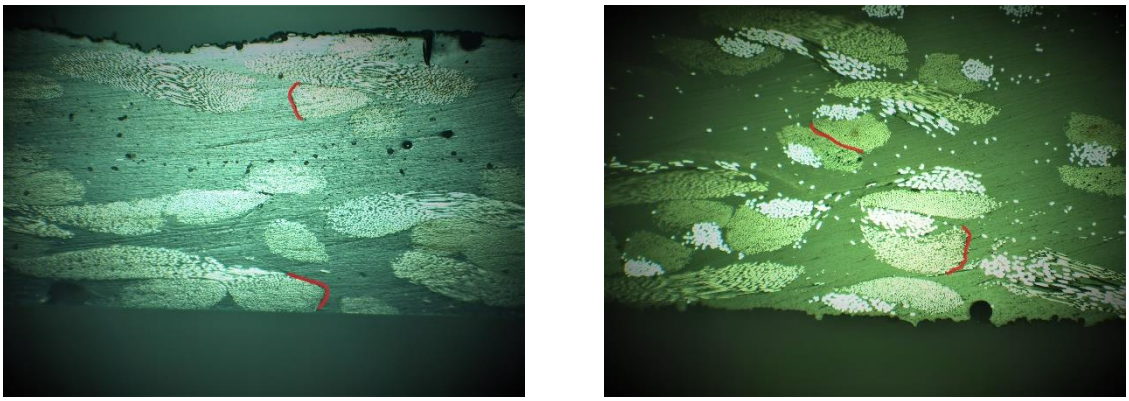

(a) (b)

Figure 5: Damage initiation in knitted composites – (a) C1 (0.6% applied strain, 50x) and (b) H1(0.6% applied strain, 50x). Transverse and shear cracks are highlighted with red.

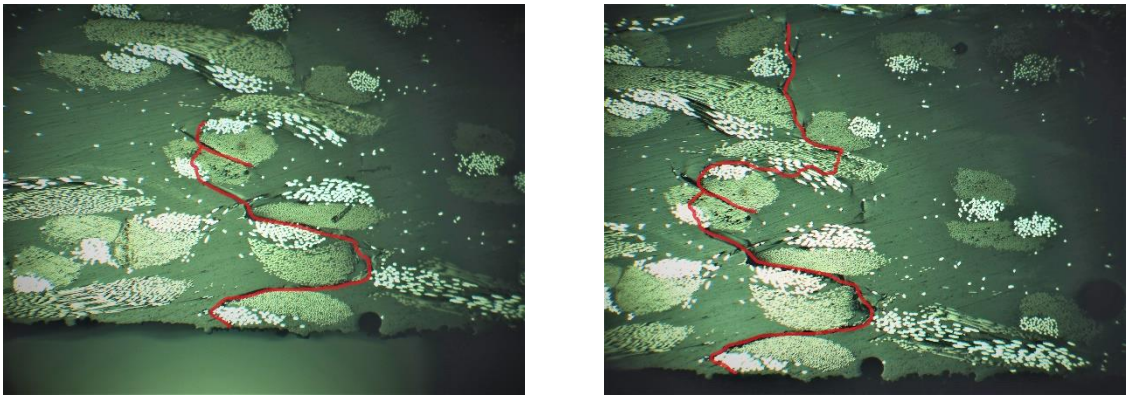

(a) (b)

Figure 6: Damage propagation in knitted composites – (a) H1 (1.0% applied strain, 50x) and (b) H1 (1.2% applied strain, 50x). Transverse and shear cracks are highlighted in red.

3.3 Micro-damage initiation and propagation – Woven composites

In the case of woven composites, damage initiation was observed at 0.8% applied strain. In CF/EP

reference materials and in hybrid composites, transverse cracks appeared at CF weft yarn boundaries and shear cracks appeared through SF weft yarns. This is shown in Fig. 7. Fig. 8 shows damage propagation in CF/EP woven reference materials. An interesting observation is shown in Fig. 8(b), where local delaminations are connected by fiber breakage of the warp yarn.

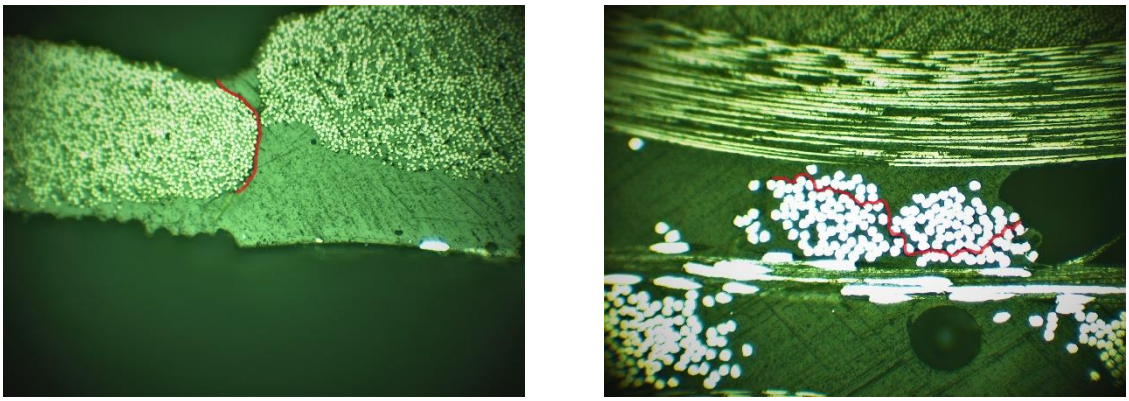

(a) (b)

Figure 7: Damage initiation in woven composites – (a) H8 (0.8% applied strain, 200x) (b) H9 (0.8% applied strain, 200x). Transverse and shear cracks are highlighted in red.

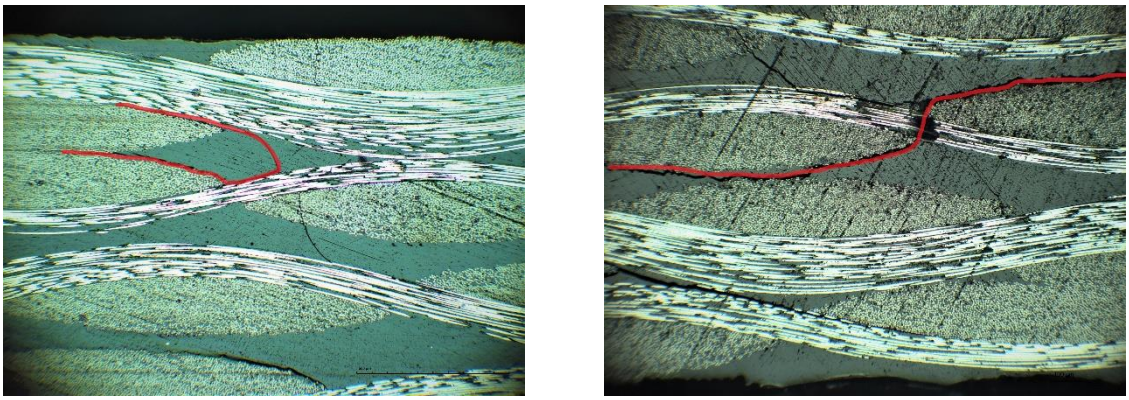

(a) (b)

Figure 8: Damage propagation in woven composites – (a) C4 (local delamination growth constrained by warp yarn, 0.8% applied strain, 100x) and (b) C4 (delaminations connecting after fiber breakage, 0.8% applied strain, 100x). Delaminations are marked in red.

3.4 Stiffness reduction

One of the major consequences of micro-damage accumulation in textile composites is reduction in stiffness along the loading direction. Fig. 9 shows trends in Ex with increase in applied strain levels for knitted and woven composites. The values on the vertical axis are normalized according to the respective undamaged material modulus for each material (refer Fig. 4), so that trends in different materials can be easily compared. Stiffness reduction is not seen in CF/EP reference material C1. A non-noticeable stiffness reduction in CF fabric reinforced composite is also reported in [7] due to low mismatch in transverse stiffness values between polymer matrix and carbon fibers. A prominent decrease in stiffness is observed for SF/EP reference material M1, knitted hybrids (H1, H2) and woven hybrids (H5, H6).

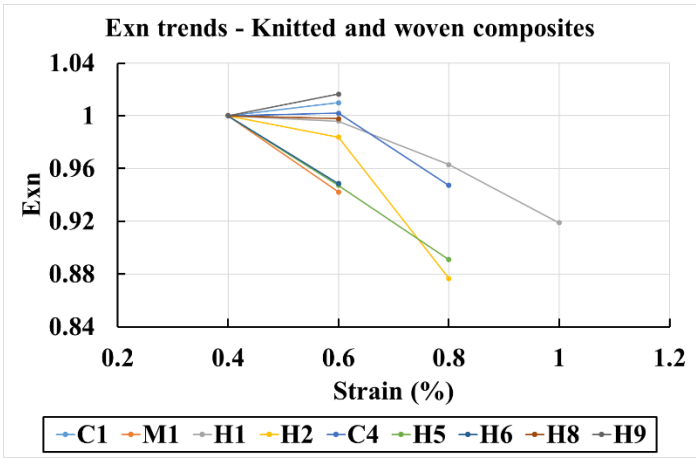

Figure 9: Ex trends for knitted and woven composites

3.5 Ultimate failure

Ultimate failure of knitted and woven specimens was characterized by multiple delaminations, and transverse cracks connected across layers through fiber breakage in warp yarns. This is depicted in Fig. 10, which shows fractured edges of C1 (knitted CF/EP reference material) and H8 (woven hybrid material). Fracture surfaces were also observed under scanning electron microscope. Fig. 11 shows SEM image of H9, which is a woven hybrid with alternate layers of CF and SF yarns. In Fig. 11, carbon- and steel fibers can be distinguished by their different sizes and shapes. Carbon fibers are smaller and round-shaped, whereas steel fibers are bigger, and polygon-shaped. The difference in the nature of fiber-matrix interfaces between carbon fibers and steel fibers is also noticeable.

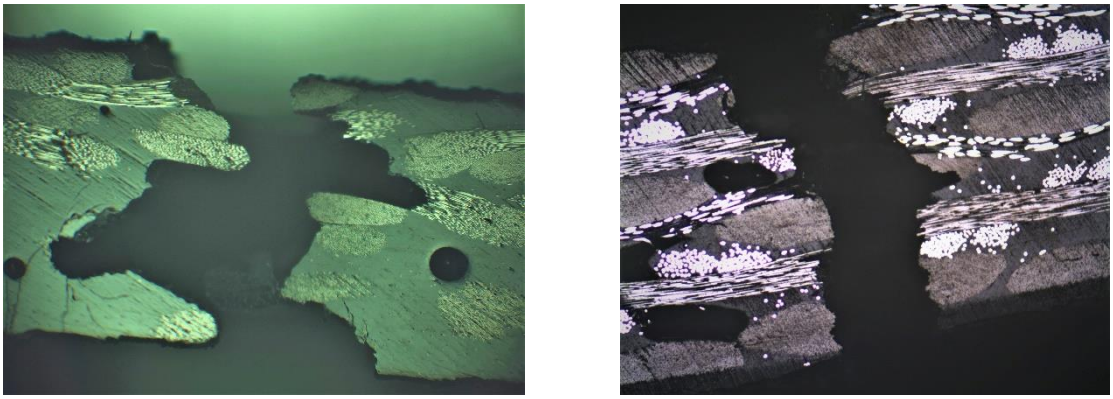

(a) (b)

Figure 10: Fractured edges after ultimate failure – (a) C1 (1.0% strain-to-failure, 50x) and (b) H8 (1.0% strain-to-failure, 50x)

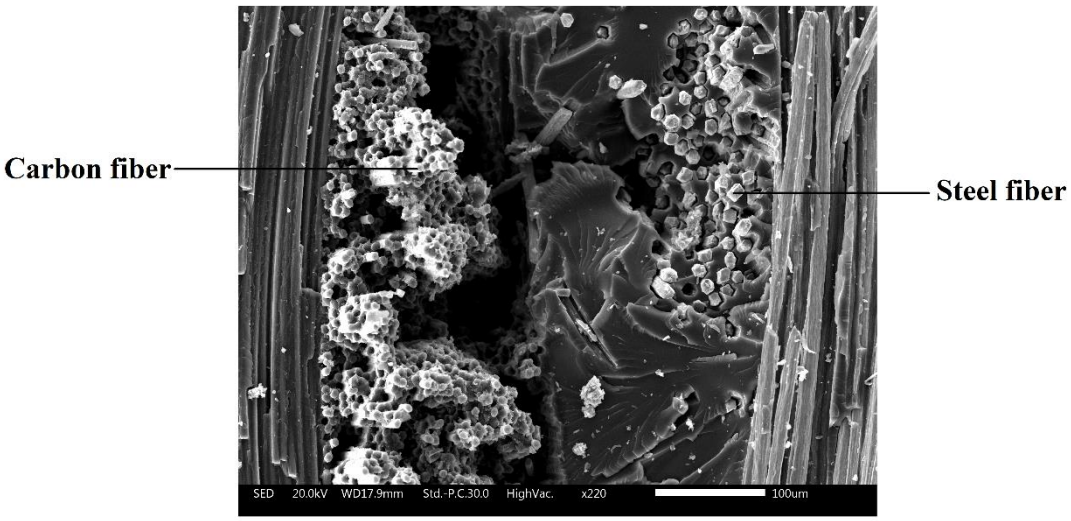

Figure 11: SEM image of fracture surface of H9 (1.0% strain-to-failure)

3.6 Strength and strain-to-failure measurements

After ultimate failure of each specimen, its strength (σmax) along loading direction and strain-to-failure (εmax) were measured. Fig. 12-13 show comparison of σmax and εmax among different types of composites. σmax comparison (refer Fig. 12) for knitted and woven composites shows a very similar trend to Ex comparison (refer Fig. 4). In the case of knitted composites, yarn-hybrid H1 has strength similar to CF/EP reference material C1 and layer-hybrid composite H2 has strength similar to SF/EP reference materials M1 and M2. In the case of woven composites, H5 with CF warp yarns has strength equivalent to CF/EP reference material C4, whereas H6 with SF warp yarns has strength equivalent to SF/EP reference materials M4 and M5.

εmax comparison (refer Fig. 13) shows that yarn-hybrid H1 has the highest strain-to-failure among all knitted and woven configurations. Such behavior signifies enhanced damage tolerance due to CF-SF yarn hybridisation. In woven configurations, all composite types have failure strains between 0.8% and 1.0% except SF/EP reference materials M4 and M5 and hybrid material H7. The cause of low failure strains in SF/EP reference materials can be the weak fiber-matrix interface which was observed in SEM images of fracture surfaces (refer Figure 11). Anomalous behavior of H7 was caused by macro-scale imperfections which arose during its manufacturing process. Efforts will be made to minimise such imperfections in the future work.

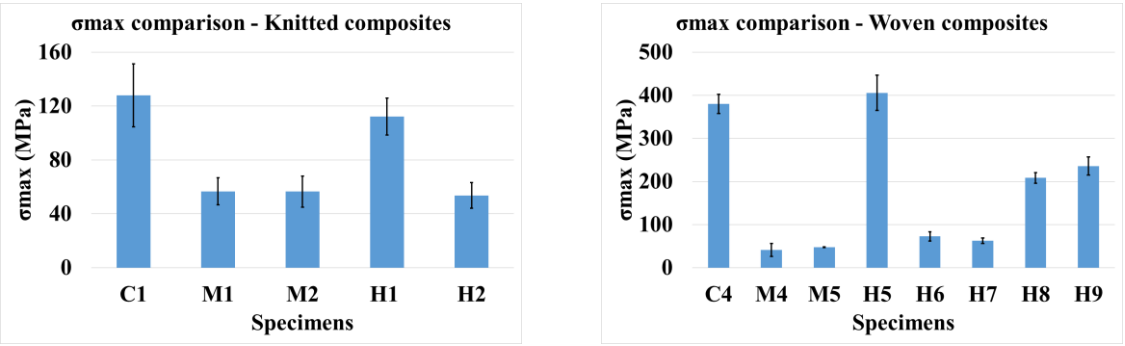

Figure 12: σmax comparison – Knitted and woven composites

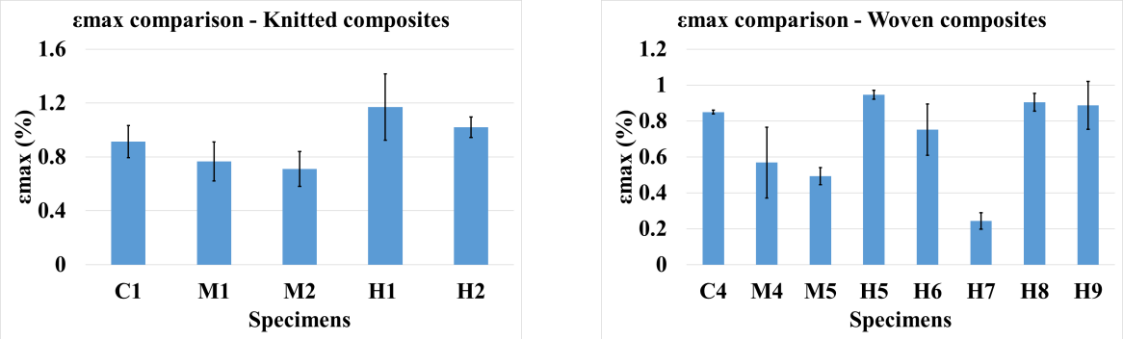

Figure 13: εmax comparison – Knitted and woven composites

4 CONCLUSIONS

Multiple configurations of hybrid carbon/steel fabric reinforced epoxy composites were tested under quasi-static tensile loading and their mechanical properties were compared with non-hybrid reference materials. The tests were performed in repetitive loading-unloading cycles with increase in maximum applied strain during each cycle. Stiffness along loading direction was measured for undamaged materials and the reduction in stiffness was observed as a result of damage accumulation. Between each test cycle, polished edges of test specimens were observed under optical microscope to study microdamage initiation and propagation.

For knitted and woven composites, microdamage initiated in the form of transverse cracks at the yarn boundaries of carbon fiber yarns and in the form of shear matrix cracks through steel fiber yarns. Propagation of delaminations along weft yarn boundaries in woven composites was arrested by warp yarns. At macro-level, knitted composites with hybrid yarns showed promising results in terms of strength and stiffness when compared with knitted composites with hybrid layers. Woven hybrid composites with carbon fibers as warp yarns had better properties than hybrids with steel fibers as warp yarns.

ACKNOWLEDGEMENTS

This work has been supported by Latvian Council of Science, project LZP-2019/1-0357 “Development and behavior analysis of novel textile composite/metal joints with enhanced mechanical properties” and the European Social Fund within the Project No 8.2.2.0/20/I/008 “Strengthening of PhD students and academic personnel of Riga Technical University and BA School of Business and Finance in the strategic fields of specialization” of the Specific Objective 8.2.2 “To Strengthen Academic Staff of Higher Education Institutions in Strategic Specialization Areas” of the Operational Programme “Growth and Employment”.

REFERENCES

[1] U. Leischner and A. F. Johnson, Micromechanics analysis of hybrid woven fabric composites under tensile and compression load, *WIT Transactions on Engineering Sciences*, **4**, 1970, pp. 397-405 (doi: 10.2495/CP940451).

[2] Ph. Vandeurzen, J. Ivens and I. Verpoest, A three-dimensional micromechanical analysis of woven-fabric composites: I. Geometric analysis, *Composites Science and Technology*, **56(11)**, 1996, pp. 1303-1315 (doi: 10.1016/S0266-3538(96)00092-9).

[3] Ph. Vandeurzen, J. Ivens and I. Verpoest, A three-dimensional micromechanical analysis of woven-fabric composites: II. Elastic analysis, *Composites Science and Technology*, **56(11)**, 1996, pp. 1317-1327 (doi: 10.1016/S0266-3538(96)00091-7).

[4] B.H. Le Page, C.I.C. Manger, F.J. Guild, S.L. Ogin and P.A. Smith, Modelling effect of layer shift on properties of woven fabric composites, *Plastics, Rubber and Composites*, **31(9)**, 2002, pp. 385-391 (doi: 10.1179/146580102225006413).

[5] B.H. Le Page, F.J. Guild, S.L. Ogin and P.A. Smith, Finite element simulation of woven fabric composites, *Composites Part A: Applied Science and Manufacturing*, **35(7-8)**, 2004, pp. 861-872 (doi: 10.1016/j.compositesa.2004.01.017).

[6] K. Kim, J.I. Curiskis, L. Ye, S. Fu, Mode-I interlaminar fracture behaviour of weft-knitted fabric reinforced composites, *Composites Part A: Applied Science and Manufacturing*, **36(7)**, 2005, pp. 954-964.

[7] L. Gorbatikh and S.V. Lomov, *Damage accumulation in textile composites*, Modeling Damage, Fatigue and Failure of Composite Materials, In Woodhead Publishing Series in Composites Science and Engineering, Woodhead Publishing, Cambridge, 2016.

[8] L. Wang, J. Wu, C. Chen, C. Zheng, B. Li, S.C. Joshi and K. Zhou, Progressive failure analysis of 2D woven composites at the meso-micro scale, *Composite Structures*, **178**, 2017, pp. 395-405 (doi: 10.1016/j.compstruct.2017.07.023).

[9] S.V. Lomov, D.S. Ivanov, T.C. Truong, I. Verpoest, F. Baudry, K. Vanden Bosche and H. Xie, Experimental methodology of study of damage initiation and development in textile composites in uniaxial tensile test, *Composites Science and Technology*, **68(12)**, 2008, pp. 2340-2349 (doi: 10.1016/j.compscitech.2007.07.005).

[10] M. Ravandi, A. Moradi, S. Ahlquist and M. Banu, Numerical Simulation of the Mechanical Behavior of a Weft-Knitted Carbon Fiber Composite under Tensile Loading, *Polymers*, **14(3)**, 2022, 451

[11] Q. Liu, J. Ma, L. Kang, G. Sun and Q. Li, An experimental study on fatigue characteristics of CFRP-steel hybrid laminates, *Materials & Design*, **88**, 2015, pp. 643-650, (doi: 10.1016/j.matdes.2015.09.024).

[12] J. Jahn, M. Weeber, J. Boehner and R. Steinhilper, Assessment Strategies for Composite-metal Joining Technologies – A Review, *Proceedings of the 26th CIRP Design Conference 2016 Vol. 50 (Eds. L. Wang, T. Kjellberg), Stockholm, Sweden, June 15-17, 2016*, Elsevier B.V., 2016, pp. 689-694.

[13] A.M. Joesbury, P.A. Colegrove, P.V. Rymenant, D.S. Ayre, S. Ganguly and S. Williams, Weld-bonded stainless steel to carbon fibre-reinforced plastic joints, *Journal of Materials Processing Technology*, **251**, 2018, pp. 241-250 (doi: 10.1016/j.jmatprotec.2017.08.023).

[14] M. Pawlik, L.Y.Y. Cheah, U. Gunputh, H. Le, P. Wood and Y. Lu, Surface engineering of carbon fibre/epoxy composites with woven steel mesh for adhesion strength enhancement, *International Journal of Adhesion and Adhesives*, 114, 2022, 103105 (doi: 10.1016/j.ijadhadh.2022.103105).

[15] A. Pupurs, I. Bramane, I. Ļašenko, M. Maniņš, M. Irbe and A. Šņepts, Manufacturing and Experimental Testing of Composite/Metal Joints with Textile Mesostructure, *ECCM 2022 - Proceedings of the 20th European Conference on Composite Materials: Composites Meet Sustainability Vol. 2 (Eds. A.P. Vassilopoulos, V. Michaud), Lausanne, Switzerland, June 26-30, 2022*, Ecole Polytechnique Fédérale de Lausanne (EPFL), Lausanne, 2022, pp. 540-546.